Transparent conductive graphene films prepared by hydroiodic acid and thermal reduction*

Qin Meng-Meng(秦盟盟), Ji Wei(纪 伟), Feng Yi-Yu(冯奕钰), and Feng Wei(封 伟)†

School of Materials Science and Engineering, Tianjin University, Tianjin 300072, *China*

(Received 31 March 2013; revised manuscript received 29 May 2013; published online 10 December 2013)

Transparent conductive graphene films are fabricated by the transfer printing of graphene aqueous dispersion followed by hydrohalic acids and thermal reduction. Results indicate that the graphene film reduced by hydroiodic acid (HI) reduction combined with thermal treatment shows a higher electrical conductivity than that reduced only by thermal treatment at the same transparency. A film with a sheet resistance of $\sim$ 2400 Ω/sq at a transparency over 72% is obtained at a typical wavelength of 550 nm.

Keywords: graphene, hydroiodic acid, thermal reduction, sheet resistance

PACS: 81.05.ue, 81.05.U–, 68.65.Pq **DOI:** 10.1088/1674-1056/23/2/028103

1. Introduction

Owing to its unique two-dimensional structure, remarkable electrical conductivity, and optical transmittance to visible and near-infrared light, graphene is promising to be an ideal material for use as transparent conductive films (TCFs), replacing traditional indium tin oxide (ITO).[1–3] TCFs based on graphene oxide (GO) obtained by chemical exfoliation are of great value in large-scale and low-cost production, since they can be easily assembled into films by well-established processes such as vacuum filtration,[4] dip-coating,[5] spray coating,[6] and the Langmuir–Blodgett[7] film technique. However, due to the disruption of graphitic networks, oxygen-containing functional groups attached to GO make the assembled film almost insulating.[8] Therefore, a deoxygenating process must be followed.[9,10]

Several methods can be utilized to deoxygenate GO, including high temperature thermal annealing[11,12] and low temperature chemical reduction.[13] Generally, the former is effective for high C/O atomic ratio, but usually needs a temperature above 1000 °C, while the latter can be conducted at a temperature lower than 100 °C, which is extremely important for practical applications.[13] Recently, Song *et al.*[14] studied the effect of thermal treatment on the structure of graphite oxide material, indicating that the oxygen-rich GO layers were rearranged into highly ordered hexagonal carbon lattices after high-temperature treatment. Pei *et al.*[13] presented a simple, highly-effective reduction method of GO films using hydroiodic acid (HI), and the film prepared shows a higher electrical conductivity and C/O atomic ratio, as well as good flexibility and structural integrity. The combination of the thermal and chemical reduction has also been reported. Wang *et al.*[15] prepared the hydrazine-reduced graphene TCFs followed by thermal treatment, and the resulting graphene film possessed a lower sheet resistance with a high transparency. Similarly, Zheng *et al.*[16] prepared the Langmuir–Blodgett TCFs consisting of ultra-large graphene sheets, and obtained a remarkable sheet resistance of 500 Ω/sq at 90% transparency after thermal reduction and chemical doping treatments.

Both thermal annealing and HI reduction can be used to reduce GO into graphene films. However, the treatment on GO through HI reduction combined with high temperature thermal annealing has not been reported. In this report, graphene TCFs are fabricated by HI and thermal reduction. Results demonstrate that the as-prepared TCF shows a higher electrical conductivity than that reduced only by thermal treatment at the same transmittance.

2. Experiment

2.1. Preparation of GO sheets

Graphene oxide was prepared using the modified Hummers method[17] from graphite flakes. Graphite (2 g) and $NaNO_3$ (2 g) were mixed in 92-mL concentrated H_2SO_4 at 0 °C. The 12-g $KMnO_4$ was gradually added into the above mixture with stirring in an ice–water bath. The mixture was first stirred at 0 °C for 2 h and then at 35 °C for 2 h. Distilled water (80 mL) was slowly added to dilute mixture over around 30 min. Then 200-mL distilled water and 10-mL H_2O_2 (30%) were added to the mixture sequentially, and the stirring continued for 30 min to obtain a graphite oxide suspension. The graphite oxide deposit was collected by high-speed centrifugation, and repeatedly washed with diluted H_2SO_4 and distilled water until the pH = 7 was reached. A mild sonication

*Project supported by the National Key Basic Research Program of China (Grant Nos. 2012CB626800 and 2010CB934700) and the National Natural Science Foundation of China (Grant Nos. 51073115, 51003072, 51173127, and 51273144).

†Corresponding author. E-mail: weifeng@tju.edu.cn

© 2014 Chinese Physical Society and IOP Publishing Ltd

(100 W, 20 min) was used to exfoliate the graphite oxide to obtain a GO suspension. Low-speed centrifugation at 2000 rpm was used to remove thick multilayers. The supernatant was further centrifuged at 4000 rpm for 5 min to separate large flakes (precipitate) from small flakes (supernatant). Finally, the obtained precipitates containing large flakes were dried in a vacuum oven at 60 °C for 24 h.

2.2. Fabrication of GO films

Substrates of graphene films were 20 mm×20 mm square quartz slides washed with deionized water, acetone, and ethanol, orderly, and then the clean substrates were dried in a vacuum at 60 °C for 24 h. The GO films were fabricated through a vacuum filtration method. The thickness of the films was controlled by varying the volumes of colloids. The filtration membranes, whose surfaces the graphene films had been deposited on, were pasted onto the quartz substrates with the film surfaces facing the substrate surface. After the films were fully dried on the substrates, the filtration membranes were dissolved in acetone, leaving the transparent graphene films on the substrates.

2.3. Reduction of GO films

Two methods were used to reduce GO films respectively. One method was to perform direct 1100 °C thermal annealing ($RGO_{1100\,^{\circ}C}$). The films were heated to 1100 °C at a rate of 10 °C/min and the temperature was held constant at 1100 °C for 1 h. To avoid burning the graphene films at such a high temperature, the furnace was purged with a mixture of hydrogen and argon for the whole process of heat treatment. The other method was to combine HI reduction with 400 °C, 700 °C, 1100 °C thermal annealing ($RGO_{HI+1100\,^{\circ}C}$), and the films were treated as follows. Before thermal annealing, the films were immersed in an HI aqueous solution (45%) at 100 °C for 100 s, and then washed repeatedly with ethanol to remove the residual HI. To further remove the residual oxygen functional groups and thus improve the electrical conductivity, the as-produced graphene films were heat treated as above.

3. Results and discussion

3.1. Surface morphology of GO sheet

Figure 1 shows the typical AFM image of GO sheet. The height curve (inset) indicates that the thickness of GO sheet is about 0.8 nm, which is thicker than the theoretical thickness of graphene (0.34 nm), due to the epoxy, carboxyl, and hydroxyl groups existing on the edges.[18] At the same time, it also indicates that the graphite oxide is almost completely exfoliated into individual graphene oxide sheets.

Figure 2 shows the typical scanning electron microscopy (SEM) image of the GO sheet. The homogeneous GO film exhibits numerous mesoscopic corrugations and wrinkles on the surface. The folded and rich-wrinkled layer morphology could improve the cross section of GO film and the electrode active area, which make the stable and uniform GO film an ideal candidate for electrode application.[19]

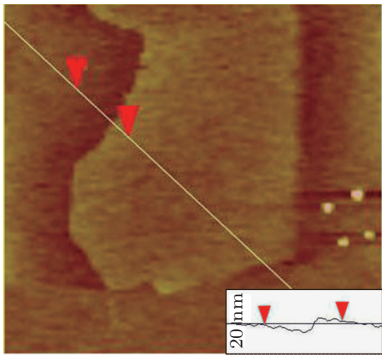


Fig. 1. (color online) AFM image of GO sheet.

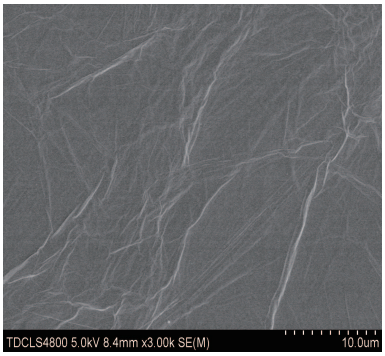


Fig. 2. (color online) SEM image of GO sheet.

Figure 3 shows the typical transmission electron microscopy (TEM) image of the graphene collected from the graphene suspension prior to the filtration. It shows a wrinkled silk-like structure in low magnification. The corrugation of the GO sheet is attributed to the disruption of the planar sp^2 carbon sheet by the introduction of sp^3-hybridized carbon upon oxidation.[20] Additionally, single-layer graphene is observed at the edge of the as-prepared graphene in high magnification. The selected area electron diffraction (SAED) pattern in the inset indicates a crystalline structure.

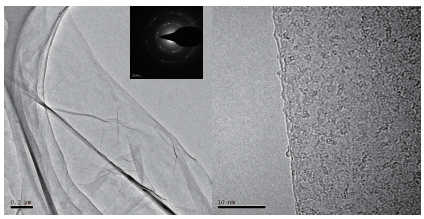


Fig. 3. (color online) TEM image of GO sheet.

3.2. Surface chemistry of GO sheet

Figure 4 shows the X-ray diffraction (XRD) patterns of pristine GO and reduced graphene sheets treated under different conditions. The diffraction peaks of the pristine GO

appear at around $2\theta = 11.18°$, corresponding to the (0 0 2) reflection of GO film. The interlayer spacing calculated from the (0 0 2) reflection is 0.79 nm, far larger than that of graphite (0.334 nm). Indeed, the large expansion of d_{002} is caused by the insertion of an oxygen-containing functional group and H_2O molecules.[21] When GO was reduced by HI (RGO_{HI}), the (0 0 2) peak was found to shift toward larger diffraction angles, corresponding to the interlayer distance decreasing from 0.79 nm to 0.369 nm, which is due to the removal of oxygen-containing functional groups. The (0 0 2) peaks of $RGO_{1100\ ^\circ C}$ and $RGO_{HI+1100\ ^\circ C}$ shift to 26.16° and 26.34°, corresponding to the interlayer distances of 0.340 nm and 0.338 nm respectively. Based on the change of the interlayer spacing, it was obtained that the $RGO_{HI+1100\ ^\circ C}$ has a minimum interlayer spacing, indicating that HI reduction combined with 1100 °C thermal annealing is more effective than the direct 1100 °C thermal treatment to some extent.

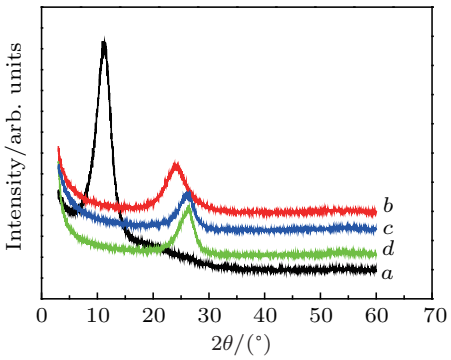


Fig. 4. (color online) XRD spectra of the as-prepared GO (curve *a*), RGO_{HI} (curve *b*), $RGO_{1100\ ^\circ C}$ (curve *c*), $RGO_{HI+1100\ ^\circ C}$ (curve *d*) sheets.

Raman spectra of GO and RGO are shown in Fig. 5. The G-band is Raman-active for sp^2-hybridized carbon-based material, while the D-band is activated only if defects participate in the double resonance Raman scattering near the *K* point of the Brillouin zone.[22] Besides G and D bands, there are two Raman bands, called 2D and D+G at 2600 cm^{-1}–3000 cm^{-1}, which are often ignored due to their weak intensities compared with D and G bands.[23] The 2D band is Raman-active for crystalline graphitic materials and is sensitive to the π-band in the graphitic electronic structure, while the combination mode of D+G is induced by disorder.[23] It is very easy to distinguish between the electronic conjugations of GO and RGO by comparing these two bands. A higher intensity ratio I_{2D}/I_{D+G} indicates better electronic conjugation, and the values of intensity ratio I_{2D}/I_{D+G} of GO, RGO_{HI}, $RGO_{1100\ ^\circ C}$, and $RGO_{HI+1100\ ^\circ C}$ are 0.93, 1.35, 1.46, and 1.83, respectively. The increased intensity ratio indicated that more graphitic electronic conjugations were recovered for $RGO_{HI+1100\ ^\circ C}$, demonstrating that HI reduction combined with thermal annealing is more effective for the reduction than that by the thermal treatment only.

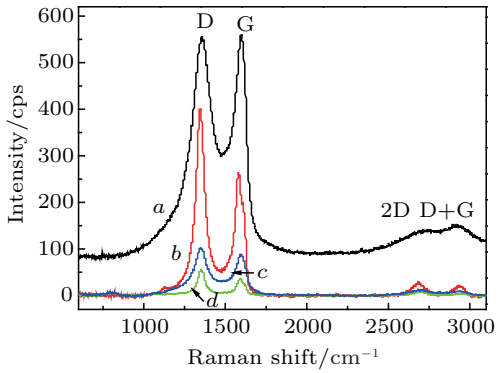


Fig. 5. (color online) Raman spectra of GO (curve *a*), RGO_{HI} (curve *b*), $RGO_{1100\ ^\circ C}$ (curve *c*), $RGO_{HI+1100\ ^\circ C}$ (curve *d*) sheets.

X-ray photoelectron spectroscopy (XPS) analysis was employed to investigate the elemental compositions of the GO sheet before and after the treatment for the understanding of surface chemistries. Figure 6 provides the C 1s XPS spectra of GO film before and after treatment. The components at

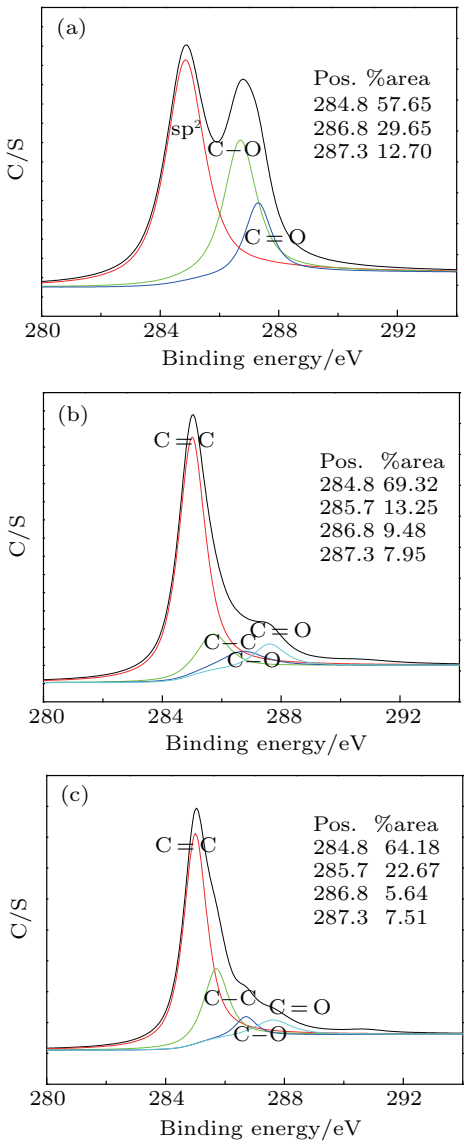


Fig. 6. (color online) High-resolution XPS C 1s spectra of GO (a), $RGO_{1100\ ^\circ C}$ (b), $RGO_{HI+1100\ ^\circ C}$ (c) films.

284.8 eV, 285.7 eV, 286.8 eV, 287.6 eV are related to C=C, C–C, C–O, C=O, respectively.[6,24] A comparison of the C/O change of GO sheet between before and after the treatment is summarized in Table 1. The C/O ratio increases with the reduction because of the removal of the oxygen-containing functional groups, and the much lower oxygen concentration in the $RGO_{HI+1100\ ^\circ C}$ film indicates the higher reduction degree of $RGO_{HI+1100\ ^\circ C}$, which is consistent with the Raman test.

Table 1. C/O changes of GO film before and after treatment.

Element	C/wt%	O/wt%	C/O
GO	70.68	26.68	2.65
$RGO_{1100\ ^\circ C}$	95.53	4.47	21.37
$RGO_{HI+1100\ ^\circ C}$	96.24	3.76	25.6

3.3. Sheet resistance of the graphene TCFs

Figure 7 shows the plots of sheet resistances of graphene films versus transparency and film thickness after different treatments. It is clearly seen that the sheet resistance gradually increases as transparency increases, suggesting a positive relationship between the sheet resistance and optical transparency. Obviously, the sheet resistance decreases with the increasing of film thickness, which was attributed to the improved structure of GO films.[15,25] Meanwhile, it is clearly indicated that the $RGO_{HI+1100\ ^\circ C}$ TCFs have relatively low sheet resistance compared with $RGO_{1100\ ^\circ C}$ TCFs at the same transmittance. Indeed, by calculating sheet resistance versus transparency at 550-nm wavelength of our films, we find that the 78.7-nm thick $RGO_{HI+1100\ ^\circ C}$ TCF shows a sheet resistance of $\sim$ 2400 Ω/sq at a transmittance of 72%, while $RGO_{1100\ ^\circ C}$ TCF reveals a sheet resistance of 3600 Ω/sq at the same transmittance. The relatively good conductivity for $RGO_{HI+1100\ ^\circ C}$ TCF is mainly because of the higher reduction degree of $RGO_{HI+1100\ ^\circ C}$. This result has practical importance in the applicable TCFs which can be obtained by controlling the thickness to balance two properties. Nevertheless, the sheet resistance of the $RGO_{HI+1100\ ^\circ C}$ TCF is still high, owing to the small size of as-prepared GO, which results in high intersheet contact resistance due to a large number of intersheet junctions.[26,27]

Figure 8 shows three groups of films with different transparencies, which include hydroiodic acid plus 400-°C annealing ($RGO_{HI+400\ ^\circ C}$), 700-°C annealing ($RGO_{HI+700\ ^\circ C}$), and 1100-°C graphitization ($RGO_{HI+1100\ ^\circ C}$), and the comparison among their sheet resistances. The figure clearly shows a trend in the electrical properties of films reduced by different methods, with sheet resistance decreasing in the order of $RGO_{HI+400\ ^\circ C}$, $RGO_{HI+700\ ^\circ C}$, $RGO_{HI+1100\ ^\circ C}$. The decreasing of the graphene film sheet resistance results from the effective recovering and subsequently more efficient annealing of continuous and overlapped graphene sheets by removing the oxygen-containing functional groups in GO films.[11]

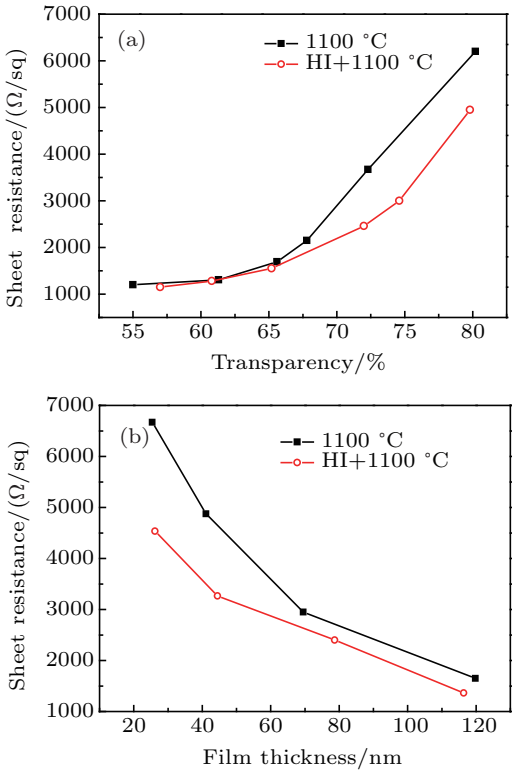


Fig. 7. (color online) Plots of sheet resistances versus transparency and film thickness of $RGO_{1100\ ^\circ C}$ and $RGO_{HI+1100\ ^\circ C}$.

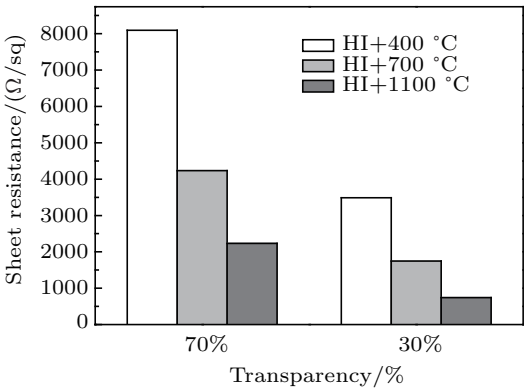


Fig. 8. Comparison among electrical properties of GO films after different reduction treatments.

Figure 9 is an optical image of a series of GO films fabricated on quartz slides, where the leftmost sample is an unreduced GO film and the others are RGO reduced by different methods. There is an obvious transmission difference between the unreduced and reduced films. The darkening films of RGO_{HI} (b) and $RGO_{HI+1100\ ^\circ C}$ (c) suggest partial restoration of the π-electron system in GO film. It is noteworthy that the $RGO_{HI+1100\ ^\circ C}$ TCF became light-colored because of the loss of material during the thermal treatment, which benefits the transparency. What is more, it could be obtained that the GO film maintained its good integrity and uniformity in the whole process.

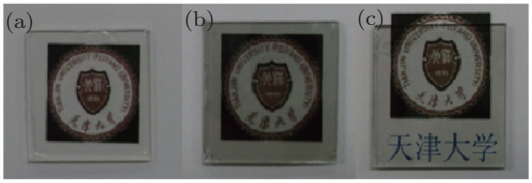


Fig. 9. (color online) Optical images of the as-prepared GO (a), RGO_{HI} (b), $RGO_{HI+1100\ ^{\circ}C}$ (c) films.

3.4. Reducing theory

The nucleophilic substitution reaction mechanism of GO film reduction by HI acid was presented by Pei *et al.*[13] as follows: (i) the ring-opening reaction of an epoxy group and (ii) the substitution reaction of a hydroxyl group by a halogen atom. Owing to the relatively good selectivity of this reaction, the reducing process can maintain good integrity of the graphene, and then it benefits the reduction of sheet resistance.

In addition, 1100 °C is known as the graphitization temperature of carbon materials[5,15,28,29] and therefore cross-linking mechanisms[15] would occur among the adjacent graphene sheets, which simultaneously restore the sp^2 C–C bonds as well as contribute to the improvement in electrical performance.[30]

4. Conclusions

A series of RGO TCFs is prepared by reducing the as-prepared GO films through direct thermal annealing and HI reduction combined with 400 °C, 700 °C, 1100 °C thermal annealings. Results show that $RGO_{HI+1100\ ^{\circ}C}$ TCF has a higher electrical conductivity than the others at the same transmittance and that $RGO_{HI+1100\ ^{\circ}C}$ TCF with a sheet resistance of $\sim 2400\ \Omega$/sq at a transparency over 72% is obtained at a typical wavelength of 550 nm. However, the sheet resistance of the $RGO_{HI+1100\ ^{\circ}C}$ TCF is still high because of the small size of as-prepared GO film. Future work will mainly aim to optimize the process of preparing GO film for obtaining large-area graphene oxide sheets or adopt the doping method to further reduce the sheet resistance.

References

[1] Novoselov K S, Geim A K, Morozov S V, Jiang D, Zhang Y, Dubonos S V, Grigorieva I V and Firsov A A 2004 *Science* **306** 666
[2] Dikin D A, Stankovich S, Zimney E J, Piner R D, Dommett G H B, Evmenenko G, Nguyen S T and Ruoff R S 2007 *Nature* **448** 457
[3] Stankovich S, Dikin D A, Piner R D, Kohlhaas K A, Kleinhammes, Jia Y Y, Wu Y, Nguyen S T and Ruoff R S 2007 *Carbon* **45** 1558
[4] Wang D W, Li F, Zhao J P, Ren W C, Chen Z G, Tan J, Wu Z S, Gentle L, Lu G Q and Cheng H M 2009 *ACS Nano* **3** 1745
[5] Becerril H A, Mao J, Liu Z F, Stoltenberg R M, Bao Z N and Chen Y S 2008 *ACS Nano* **2** 463
[6] Shin H J, Kim K K, Benayad A, Yoon S M, Park H K, Jung I S, Jin M H, Jeony H K, Kim J K, Choi J Y and Lee Y H 2009 *Adv. Funct. Mater.* **19** 1987
[7] Cote L J, Kim F and Huang J X 2009 *J. Am. Chem. Soc.* **131** 1043
[8] Mkhoyan K A, Contryman A W, Silcox J, Stewart D A, Eda G, Mattevi C, Miller S and Chhowalla M 2009 *Nano Lett.* **9** 1058
[9] Wang H L, Robinson J T, Li X L and Dai H J 2009 *J. Am. Chem. Soc.* **131** 9910
[10] Chen J Y, Zhang H L, Huang L P, Wu B, Wei D C and Liu Y Q 2009 *Physics* **38** 387 (in Chinese)
[11] Wang X, Zhi L J and Mullen K 2008 *Nano Lett.* **8** 323
[12] Fan X B, Peng W C, Li Y, Li X Y, Wang S L, Zhang G L and Zhang F B 2008 *Adv. Mater.* **20** 4490
[13] Pei S F, Zhao J P, Du J H, Ren W C and Cheng H M 2010 *Carbon* **48** 4466
[14] Song L, Khoerunnisa F, Gao W, Dou W H, Hayashi T, Kaneko K, Endo M and Ajayan P M 2013 *Carbon* **52** 608
[15] Wang S J, Geng Y, Zheng Q B and Kim J K 2010 *Carbon* **48** 1815
[16] Zheng Q B, Ip W H, Lin X Y, Yousefi N, Yeung K K, Li Z G and Kim J K 2011 *ACS Nano* **5** 6039
[17] Zhao J P, Pei S F, Ren W C, Gao L B and Cheng H M 2010 *ACS Nano* **4** 5245
[18] Chen W F, Yan L F and Bangal P R 2010 *Carbon* **48** 1146
[19] Tang L H, Feng H B, Cheng J S and Li J H 2010 *Chem. Commun.* **46** 5882
[20] Yu A P, Rose I, Davies A and Chen Z W 2010 *Appl. Phys. Lett.* **96** 253105
[21] Zhao B, Liu P, Jiang Y, Pan D Y, Tao H H, Song J S, Fang T and Xu W W 2012 *J. Power Sources* **198** 423
[22] Pimenta M A, Dresselhaus G, Dresselhaus M S, Cancado L G, Jorio A and Saito R 2007 *Phys. Chem. Chem. Phys.* **9** 1276
[23] Lee V, Whittaker L, Jayer C, Baroudi K M, Fischer D A and Banerjee S 2009 *Chem. Mater.* **21** 3905
[24] Ganguly A, Sharma S, Papakonstantinou P and Hamilton J 2011 *J. Phys. Chem. C* **115** 17009
[25] Wang X, Zhi L J, Tsao N, Tomovic Z, Li J L and Mullen K 2008 *Angew. Chem. Int. Ed.* **47** 2990
[26] Li X L, Zhang G Y, Bai X D, Sun X M, Wang X R, Wang E and Dai H J 2008 *Nat. Nanotechnol.* **3** 538
[27] Yamaguchi H, Eda G, Mattevi C, Kim H and Chhowalla M 2010 *ACS Nano* **4** 524
[28] Kim U J, Liu X M, Furtado C A, Chen G, Saito R, Jiang J, Dresselhaus M S and Eklund P C 2005 *Phys. Rev. Lett.* **95** 157402
[29] Berger C, Song Z M, Li X B, Wu X S, Brown N, Naud C, Mayou D, Li T B, Hass J, Marchenkov A N, Conrad E H, First P N and Heer W A 2006 *Science* **312** 1191
[30] Zhi L J, Wu J S, Li J, Kolb U and Mullen K 2005 *Angew. Chem. Int. Ed.* **44** 2120